Acta Zoologica (Stockholm) **80:** 47–59 (January 1999)

The ultrastructure of the spermatozoa of the lizard *Micrablepharus maximiliani* (Squamata, Gymnophthalmidae), with considerations on the use of sperm ultrastructure characters in phylogenetic reconstruction

Ruscaia D. Teixeira[1,2], Guarino R. Colli[3] and Sônia N. Báo[1]

[1]Departamento de Biologia Celular
Universidade de Brasília
70919970 Brasília
DF, Brazil
[2]Departamento de Biologia Celular
Universidade Estadual de Campinas
13083970 Campinas
SP, Brazil
[3]Departamento de Zoologia
Universidade de Brasília
70910900 Brasília
DF, Brazil
E-mail: grcolli@guarany.unb.br

Keywords:
phylogeny, spermatozoa, squamata, ultrastructure

Accepted for publication:
30 July 1998

Abstract

Teixeira, R. D., Colli, G. R. and Báo, S. N. 1999. The ultrastructure of the spermatozoa of the lizard *Micrablepharus maximiliani* (Squamata, Gymnophthalmidae), with considerations on the use of sperm ultrastructure characters in phylogenetic reconstruction. — *Acta Zoologica* (Stockholm) **80:** 47–59

We describe, for the first time, the ultrastructure of the spermatozoa of a member of the family Gymnophthalmidae. Mature spermatozoa of *Micrablepharus maximiliani* are characterized by: acrosome circular in transverse section, absence of perforatorial base plate, perforatorial tip pointed, absence of epinuclear lucent zone, midpiece short, mitochondria in transverse section forming a circlet interrupted by dense bodies, trapezoid mitochondria, dense bodies solid and arranged in regular rings and linear series, linear mitochondrial cristae, rounded nuclear shoulders, elongate nuclear shape, absence of endonuclear canal, fibers 3 and 8 enlarged, absence of multilaminar membranes, and fibrous sheath in midpiece. Phylogenetic analysis of the Squamata after the addition of the Gymnophthalmidae to the ultrastructure data set previously published by Jamieson, resulted in 8733 equally parsimonious trees that conflicted with phylogenetic hypotheses derived from morphological data sets. An analysis of tree-length distribution skewness, however, indicated that the ultrastructure data set contains significant phylogenetic information. We suggest that rates of evolution for spermatozoa ultrastructure characters might be higher than currently thought, resulting in incongruent tree topologies derived from distinct data sets. Finally, we suggest that because only optimal trees were selected, the heterogeneity between the data sets might be apparent and more analyses are necessary to evaluate the nature and degree of the heterogeneity between them.

Sônia N. Báo. Departamento de Biologia Celular, Instituto de Biologia, Universidade de Brasília, 70919970 Brasília-DF, Brazil. E-mail: snbao@unb.br

Introduction

In recent years, the ultrastructure of spermatozoa has been described for various families of Squamata (reviewed in Jamieson 1995b; Jamieson *et al.* 1996; Oliver *et al.* 1996). The development of such an extensive data set, paralleled by the utilization of spermatozoal ultrastructure characters in phylogenetic

studies of insects (Jamieson, 1987) and fishes (Jamieson, 1991), has naturally led to phylogenetic analyses of squamates based on the ultrastructure of spermatozoa (Jamieson, 1995b; Jamieson *et al.* 1996; Oliver *et al.* 1996). These analyses revealed, on the one hand, strong support for the monophyly of Squamata and, on the other, major incongruencies between phylogenies derived from sperm ultrastructure and those derived from morphological characters (Estes *et al.* 1988; Russel 1988; Schwenk 1988; Maddison and Maddison 1996). For example, the Iguania, Scleroglossa, Gekkota, Scincomorpha, and Anguimorpha are not monophyletic in phylogenetic hypotheses derived from the ultrastructure of spermatozoa (Jamieson 1995b).

A common product of the increased number of data sets available for a group of taxa is the disagreement between phylogenies derived from each data set. This heterogeneity among phylogenetic reconstructions often results from sampling error, different stochastic processes acting on different data sets or portions of data sets, and different phylogenetic histories (e.g. Swofford 1991b; de Queiroz *et al.* 1995; Miyamoto and Fitch 1995). In the absence of studies that qualify the nature and degree of the heterogeneity between the morphological and sperm ultrastructure data sets from squamates, there is no reason to a priori regard either one as superior to the other in the ability to accurately reflect true phylogenetic relationships. However, data on the ultrastructure of spermatozoa of squamates still suffer from two deficiencies. First, the number of characters employed in phylogenetic analysis (Jamieson 1995b) is rather limited (17), what may lead, with the broadening of the taxonomic coverage, to the uncomfortable situation of having more taxa than character states in the study matrix. Second, the ultrastructure of spermatozoa of several families of squamates still awaits description (Jamieson 1995b).

The Gymnophthalmidae comprises an array of 30 genera that range from southern Mexico to northern Argentina (Presch 1980). The group was previously considered a subfamily of the Teiidae until Presch (1983) raised gymnophthalmines to the familial rank. Even though a closer relationship with the Lacertidae was once suggested (Presch 1983), the Gymnophthalmidae are currently believed to be the sister-taxon of the Teiidae (Estes *et al.* 1988; Schwenk 1988). Herein we describe, for the first time, the ultrastructure of the spermatozoa of a member of the family Gymnophthalmidae, *Micrablepharus maximiliani*, and make comparisons with other families of squamates. In addition, we conduct a phylogenetic analysis of the Squamata after the addition of a new family to the sperm ultrastructure data set of Jamieson (1995b), attempting to evaluate the usefulness of such characters in phylogeny reconstruction and to provide directions for future work.

Materials and Methods

Spermatozoa ultrastructure

We obtained sperm samples from an adult specimen of *Micrablepharus maximilini* collected at Minaçu, Goiás State, Brazil (13°38′ S, 48°15′ W) in February 1997. We killed the specimen with Tiopental®, removed the epididymis by dissection, placed it in a Petri dish with phosphate buffered saline (PBS) pH 7.2, and cut it into small pieces. We fixed spermatozoa and epididymal tissues overnight at 4 °C in a solution containing 2.5% glutaraldehyde, 2% paraformaldehyde, and 3% sucrose in 0.1 m sodium cacodylate buffer pH 7.2. Subsequently, we rinsed the samples in 0.1 m sodium cacodylate buffer pH 7.2 and postfixed them for 1 h in 1% osmium tetroxide, 0.8% potassium ferricyanide, and 5 mm $CaCl_2$ in 0.1 m sodium cacodylate buffer. We dehydrated the material in acetone and embedded it in Spurr's epoxy resin. We cut sections with diamond knives, on a Reichert ultramicrotome. After sectioning and staining with uranyl acetate and lead citrate, we examined and photographed sections with a Jeol® 100C transmission electron microscope at 80 kV. We made light microscopic observations of spermatozoa, from glutaraldehyde-paraformaldehyde fixed sperm smears, under Nomarski contrast using a Zeiss® Axiophot microscope.

Phylogenetic analyses

We scored *Micrablepharus maximiliani* for the 17 ultrastructural characters of squamate sperm described by Jamieson (1995b) (Table 1). Then, we built a taxon-character matrix (Table 2), by joining *M. maximiliani* to the matrix assembled by Jamieson (1995b). It should be noted that we assigned *Pogona barbata* to the Chamaeleonidae, following Frost and Etheridge (1989) in that Agaminae is a subfamily of Chamaeleonidae. We produced most parsimonious phylogenetic hypotheses using Paup vs. 3.0 s for the Macintosh (Swofford 1991a) and a branch-and-bound search, performed with the default options. We regarded all characters as unordered, and Chelonia and *Sphenodon punctatus* as a paraphyletic outgroup with respect to the ingroup. Reconstructions of character evolution were produced with MacClade v.3.06 (Maddison and Maddison 1992).

Results

Ultrastructure of spermatozoa

Spermatozoa of *Micrablepharus maximiliani* are filiform and $\approx$ 60 μm long (Figs 1, 2A). The head is short and curved, and $\approx$ 11 μm in total length, from light microscopy. The midpiece, a thick and short portion in the posterior

Table 1 Ultrastructure characters of the spermatozoa of squamates used in phylogenetic analyses. Data from Jamieson (1995b).

Character	States
1 Acrosome in transverse section	(0) circular (1) depressed
2 Perforatorial base plate	(0) absent or indistinct (1) knoblike (2) stopperlike
3 Perforatorial tip	(0) pointed (1) square ended
4 Perforatoria number	(0) two or more (1) one
5 Epinuclear lucent zone	(0) absent (1) poorly developed (2) well developed
6 Midpiece	(0) short (1) moderately long (2) very long
7 Mitochondria in transverse section	(0) regular circlet (1) not regular (2) intermediate
8 Mitochondria shape	(0) rounded (1) columnar (2) sinuous tubes (3) intermediate rounded-columnar (4) trapezoid
9 Dense bodies	(0) intramitochondrial (1) regular rings (2) scattered (3) linear series (4) stellate spiral (5) 2 groups
10 Dense bodies, if regular	(0) not applicable (1) solid (2) granular (3) single file granules
11 Mitochondrial cristae	(0) concentric (1) linear
12 Nuclear shoulders	(0) sharp (1) rounded (2) absent
13 Nuclear shape	(0) elongate (1) stout
14 Endonuclear canal	(0) present (1) absent
15 Fibers 3 and 8	(0) enlarged (1) grossly enlarged anteriorly
16 Multilaminar membranes	(0) absent (1) present
17 Fibrous sheath	(0) not in midpiece (1) in midpiece

Table 2 Comparative ultrastructure of Squamata sperm, *Sphenodon punctatus* and Chelonia. All data from Jamieson (1995b), except for *M. maximiliani*.

Taxon	Characters																
	1	2	3	4	5	6	7	8	9	10	11	12	13	14	15	16	17
Chelonia	0	0	0	0	0	0	0	0	0	0	0	0	0	0	0	0	0
Sphenodon punctatus	0	0	0	0	0	0	0	0	0	0	0	0	0	0	0	0	0
Ctenotus robustus (Scincidae)	1	0	0	1	1	0	0	1	1	1	1	1	0	1	0	0	1
Chalcides ocellatus (Scincidae)	1	0	0	1	?	0	0	1	1	3	1	1	0	1	0	0	1
Lacertidae	1	0	0	1	1	0	0	1	5	0	1	1	0	1	0	0	1
Cnemidophorus sexlineatus (Teiidae)	1	0	0	1	2	0	0	1	1	1	1	1	0	1	0	0	1
Tiliqua scincoides (Scincidae)	1	0	0	1	0	0	0	1	1	1	1	1	0	1	0	0	1
Carlia pectoralis (Scincidae)	0	1	1	1	2	1	1	2	2	0	1	0	1	1	1	0	1
Lampropholis delicata (Scincidae)	0	1	1	1	2	1	1	2	2	0	1	0	1	1	1	0	1
Heteronotia binoei (Gekkonidae)	0	2	0	1	0	1	0	1	4	0	1	1	0	1	0	0	1
Lygodactylus picturatus (Gekkonidae)	0	2	0	1	2	1	0	1	4	0	1	1	0	1	0	0	1
Lialis burtonis (Pygopodidae)	0	?	1	1	2	1	1	2	3	0	1	2	1	1	0	1	1
Pogona barbata (Chamaeleonidae)	1	1	0	1	2	0	2	3	1&3	1	1	1	0	1	0	0	1
Varanus gouldii (Varanidae)	1	1	0	1	2	0	0	1	1	2	1	1	0	1	0	0	1
Boiga irregularis & Stegonotus cucullatus (Colubridae)	0	0	0	1	1	2	1	2	3	0	1	1	0	1	0	0	1
Oxyuranus microlepidotus (Elapidae)	0	0	0	1	?	2	1	2	3	0	1	1	0	1	0	1	1
Aspidites melanocephalus (Boidae)	0	0	0	1	?	2	1	2	3	0	1	1	0	1	0	1	1
Iguanidae	0	0	0	1	2	0	0	2	1&2	1	1	0&1	0	1	0	0	1
Bradypodion karroicum (Chamaeleonidae)	1	0	0	1	2	1	0	2	2	0	1	1	0	1	0	0	1
Micrablepharus maximiliani (Gymnophthalmidae)	0	0	0	1	0	0	2	4	1&3	1	1	1	0	1	0	0	1

segment of the head, is ≈ 2.5 μm long, from transmission electron microscopy. The tail (principal piece and endpiece) is ≈ 46.5 μm long from transmission electron microscopy.

Acrosome complex. The acrosome complex consists of an external cap, the acrosome vesicle, an internal cap, the paracrystalline subacrosomal cone, and the perforatorium (Fig. 2B). In cross-section, the acrosome complex appears circular (Fig. 2D,E). The acrosome vesicle is a homogeneous and electron-dense structure that ensheathes the subacrosomal cone (Fig. 2B). A narrow central canal, the perforatorium, extends from the anterior region of the subacrosomal cone and projects into the acrosome vesicle (Fig. 2B-D). The subacrosomal cone wraps the tapered anterior end of the nucleus (Fig. 2E,F), and is separated from the acrosome vesicle by an electron-lucent space

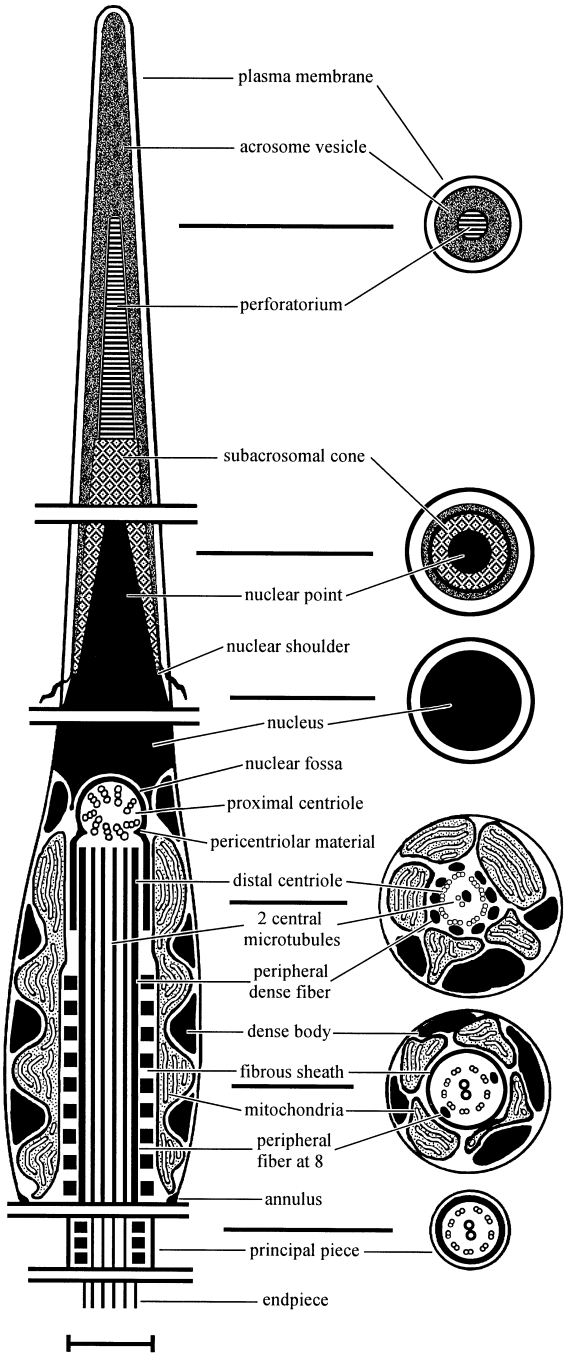

Fig. 1.—Diagram of the spermatozoa of *Micrablepharus maximiliani*, in longitudinal section and corresponding transverse sections. Scales of various components are only approximate. Scale bar 0.5 μm.

(Fig. 2C). At its posterior end, the acrosome complex lies on a postero-lateral membranous flange (Fig. 2F).

Nucleus. The nucleus is a curved cylinder, with the apical region tapering within the subacrosomal cone (Fig. 2B,F). In transverse section, the nucleus is circular (Fig. 2H,I). The chromatin is strongly electron-dense and condensed, with some electron-lucent lacunae (Fig. 2G,H). The transition from the tapered apical portion (nuclear rostrum) to the cylindrical region is abrupt and marked by small rounded 'shoulders' (Fig. 2F). At its base, the nucleus has a moderately deep nuclear fossa, that houses electron-dense material and partially covers the proximal centriole (Fig. 2I, J). The nuclear point is not capped by an electron-lucent space.

Neck region. The neck region is the transition between nucleus and midpiece. It contains the proximal and distal centrioles, the first ring of dense bodies (mitochondrial transformations) and mitochondria (Fig. 3A). The proximal centriole is transversely oriented in longitudinal section and is partially surrounded by dense pericentriolar material, that conforms in shape to the nuclear fossa and extends posteriorly between the two centrioles (Fig. 2J, 3A, B). An electron-lucent space separates the pericentriolar material from the nuclear fossa. An electron-dense laminar structure sits above the proximal centriole (Fig. 3C). The distal centriole is in the long axis of the flagellum (Fig. 3A,B) and consists of nine triplets of microtubules, nine peripheral fibers associated with the triplets, and the two central singlets of the axoneme, which extend into the posterior region of the distal centriole (Fig. 3D). One of the central microtubules is surrounded by dense material.

Midpiece. The midpiece consists of the neck region and the axoneme, surrounded by mitochondria, rings of dense bodies (mitochondria transformations) and a fibrous sheath (Fig. 3A,F). The midpiece ends posteriorly with the annulus (Fig. 3G). The axoneme is formed by a pair of central microtubules surrounded by nine doublets and nine peripheral fibers of dense material. The peripheral dense fibers associated with doublets three and eight are

Fig. 2.—Spermatozoa of *Micrablepharus maximiliani*.—**A,** Light micrograph showing whole spermatozoon with head, midpiece and flagellum.—**B-J,** Transmission electron micrographs of the head (acrosome complex and nucleus). (B) Longitudinal section of the acrosome complex surrounding the nuclear point. (C) Detail of the acrosome complex showing the perforatorium. Arrow head indicates electron-lucent space. (D-E) Transverse section of the acrosome complex at, respectively, the perforatorium and nuclear point levels. (F) Posterior region of acrosome complex with arrow heads indicating the nuclear shoulders. (G-H) Longitudinal and transverse sections, respectively, of nucleus showing the lacunae. (I-J) Basal region of nucleus and the nuclear fossa in transverse and longitudinal sections, respectively. Note the pericentriolar material. **Fig. 2**A: scale bar 10 m; Fig. 2B-J: scale bar 0.2 μm. Abbreviations: a = acrosome vesicle; an = annulus; ax = axoneme; db = dense bodies; dc = distal centriole; f = flagellum; fs = fibrous sheath; h = head; l = nuclear lacuna; ls = laminar structure; m = mitochondria; mp = midpiece; *n* = nucleus; nf = nuclear fossa; p = perforatorium; pc = proximal centriole; pf = peripheral dense fibre; pm = pericentriolar material; sc = subacrosomal cone.

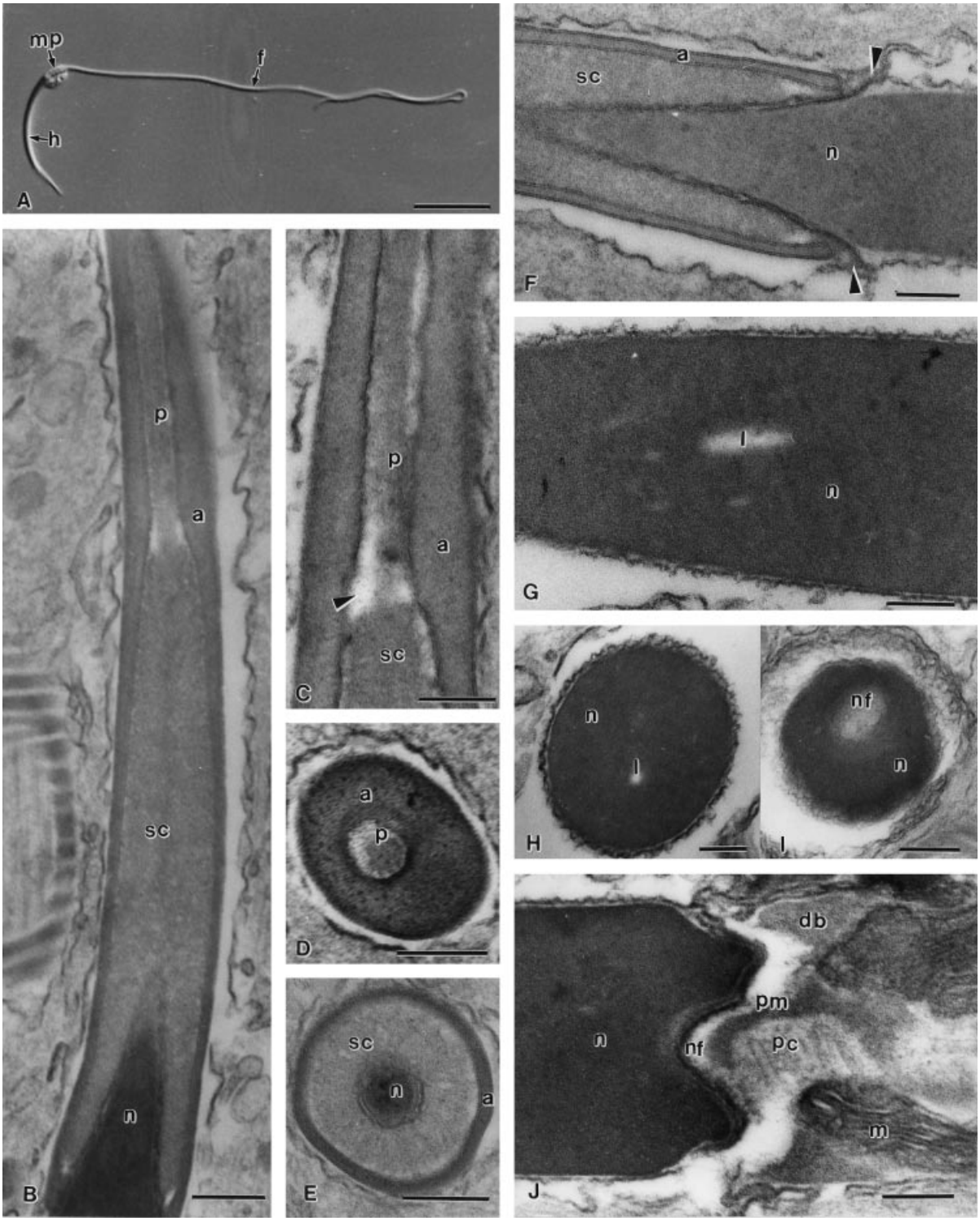

Fig. 2

thicker than the others and are separated from their corresponding doublets (Fig. 3F). The axoneme is enclosed in the fibrous sheath, formed by regularly spaced, approximately square dense blocks, connected by the longitudinal thicker peripheral fibers three and eight (Fig. 3E,F). The trapezoid mitochondria are of variable size, contain linear cristae and apparently surround the distal centriole and the fibrous sheath in a spiral fashion (Fig. 3A,B,D,F). Regularly spaced dense bodies lie in external depressions of the mitochondria, almost always separated from the centrioles and fibrous sheath by mitochondrial projections (Fig. 3A). In transverse sections of the midpiece, dense bodies are interrupted by mitochondria, hence they do not form continuous rings (Fig. 3F). At the posterior end of midpiece, the mitochondria become slender in cross section and are well separated from the fibrous sheath by cytoplasmatic material (Fig. 3G,H). The annulus appears like a very small dense ring (Fig. 3G).

Principal piece. This is the longest portion of the flagellum, consisting of the axoneme surrounded by the fibrous sheath, cytoplasm and plasma membrane (Fig. 3I). In this region, the axoneme presents a 9 + 2 microtubules pattern, and neither peripheral dense fibers can be observed (Fig. 3J). The diameter of the principal piece gradually diminishes, as a result of a decreasing cytoplasm between the fibrous sheath and the plasma membrane and a reduction in the width of the fibrous sheath.

Endpiece. The endpiece was not clearly observed.

Phylogenetic analyses

A total of 8733 alternative tree topologies were discovered (length = 47, C.I. = 0.729, R.C.I = 0.583). A strict consensus tree and a 50% majority-rule consensus tree (Miyamoto 1985) are presented in Fig. 4. It is worth emphasizing that consensus trees are often less parsimonious than the original trees from which they derive (Miyamoto 1985; Barret *et al.* 1991), thus they should not be regarded as phylogenies but rather as statements about areas of agreement among trees (Swofford 1991b). The strict consensus tree (Fig. 4A) clearly indicates a monophyletic Squamata, but it is not very informative regarding relationships among squamates, except for the monophyletic groups *Pogona barbata* + *Varanus gouldii*, another formed by an unresolved trichotomy comprising the Serpentes (*Oxyuranus microlepidotus*, *Aspidites melanocephalus*, Colubridae), skinks of the *Eugongylus* species-group (*Carlia pectoralis*, *Lampropholis delicata*), and the pygopodid *Lialis burtonis*, and a third monophyletic group comprising the Serpentes.

The 50% majority-rule tree indicates a monophyletic Squamata (Fig. 4B), supported by 9 characters (Table 3). Four clades emerge from a basal polytomy. Two of these clades contain just a single family: the Iguanidae and the Gymnophthalmidae. The third one appeared in 72% of the 8733 alternative trees and contains the Lacertidae, Scincidae (part), Teiidae, Varanidae, and Chamaeleonidae (part). This clade is basically unresolved, except for two sister-groups: Lacertidae and *Ctenotus robustus*, which is weakly supported (54%), and Varanidae and Chamaeleonidae (*Pogona barbata*), which was common to 100% of the alternative trees. The fourth clade is relatively well supported, having appeared in 81% of the most-parsimonious reconstructions. It is formed by the sequential addition of the Gekkonidae, Chamaeleonidae (*Bradypodion karroicum*), Serpentes, Pygopodidae (*Lialis burtonis*), and Scincidae of the *Eugongylus* species-group (*Carlia pectoralis*, *Lampropholis delicata*). Most of these groups were strongly supported, as indicated by the frequency of occurrence among the alternative trees, except for Chamaeleonidae (part) + Serpentes + Pygopodidae + Scincidae of the *Eugongylus* species-group (55%), and Pygopodidae + Scincidae of the *Eugongylus* species-group (56%).

Because of the presence of unresolved ('soft') polytomies (Maddison and Maddison 1992), few unambiguous character transformations could be identified (Table 3). These included the autapomorphic states in the Lacertidae (dense bodies not regular, dense bodies in 2 groups), *Varanus gouldii* (dense bodies granular), *Pogona barbata* (mitochondria intermediate in transverse section, mitochondria shape intermediate rounded-columnar), *Heteronotia binoei* (epinuclear lucent zone absent), and *Bradypodion karroicum* (acrosome depressed in transverse section), and the synapomorphic states of the Gekkonidae (stopperlike perforatorial base plate), Serpentes + Pygopodidae + Scincidae of the *Eugongylus* species-group (mitochondria not regular in transverse section), Pygopodidae + Scincidae of the *Eugongylus* species-group (perforatorial tip square-ended, nuclear shape elongate), and Scincidae of the *Eugongylus* species-group (fibers 3 and 8 grossly enlarged anteriorly).

Fig. 3.—Spermatozoa of *Micrablepharus maximiliani*. Transmission electron micrographs of the tail (midpiece and principal piece).—**A,** Longitudinal section of the midpiece.—**B,** Longitudinal section of the neck region with pericentriolar material and centrioles.—**C,** Detail of the neck region in longitudinal section, showing the laminar structure.—**D,** Transverse section of the neck region showing the distal centriole with the central singlets and peripheral fibers.—**E,** Longitudinal section of the midpiece, showing the transition between the distal centriole and the axoneme. Note the fibrous sheath surrounding the axoneme.—**F,** Transverse section of the midpiece showing the axoneme with peripheral fibers 3 and 8 (arrow heads) enlarged and detached from their doublets.—**G-H,** Transition region between midpiece and principal piece in longitudinal and transverse sections, respectively. Note the annulus in longitudinal section.—**I-J,** Longitudinal and transverse sections, respectively, of principal piece, showing fibrous sheath and axoneme without peripheral fibers. Fig. 3A-C,E-I: scale bar 0.5 μm; Fig. 3D and J: scale bar 0.2 μm. Abbreviations as in Fig. 2.

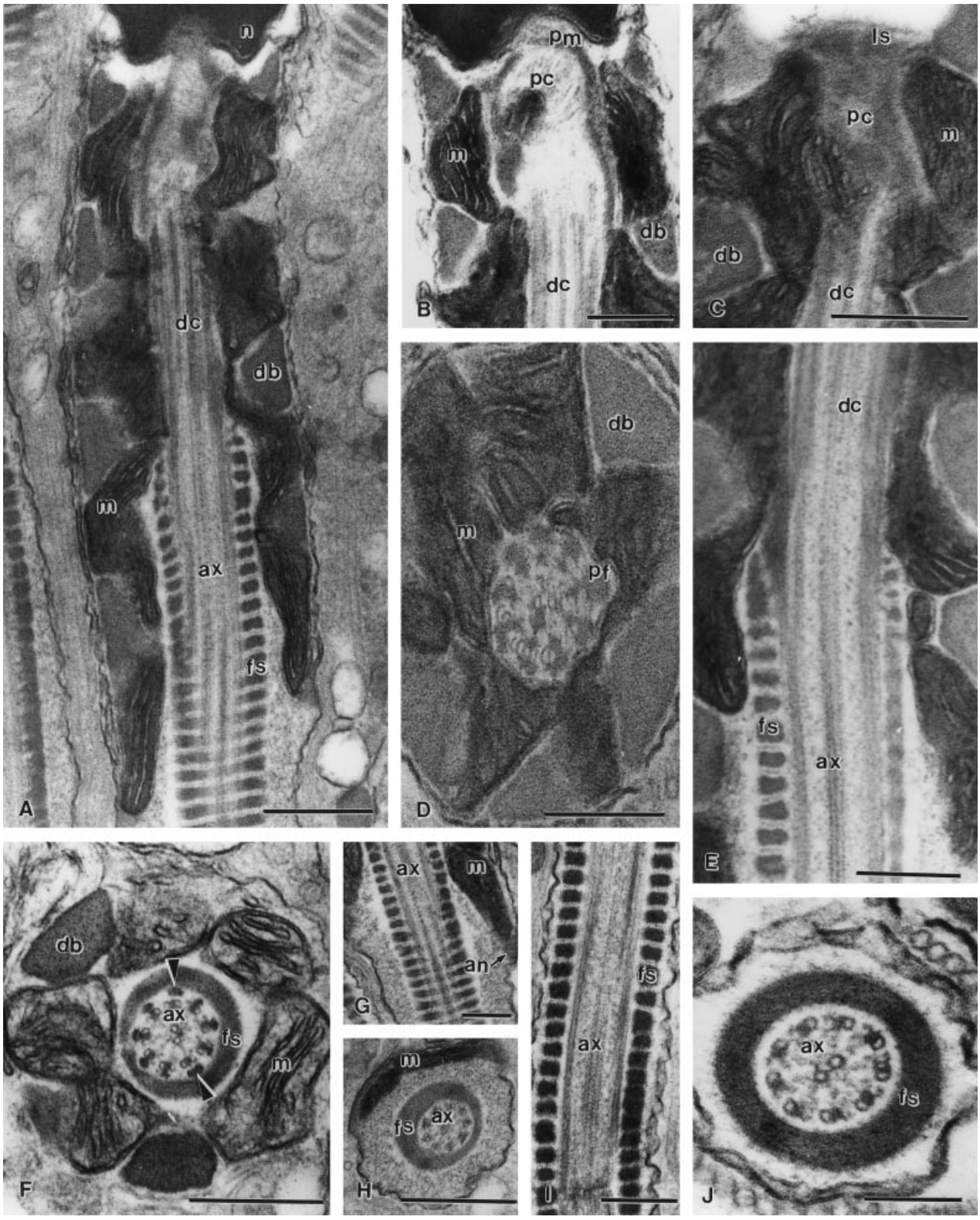

Fig. 3

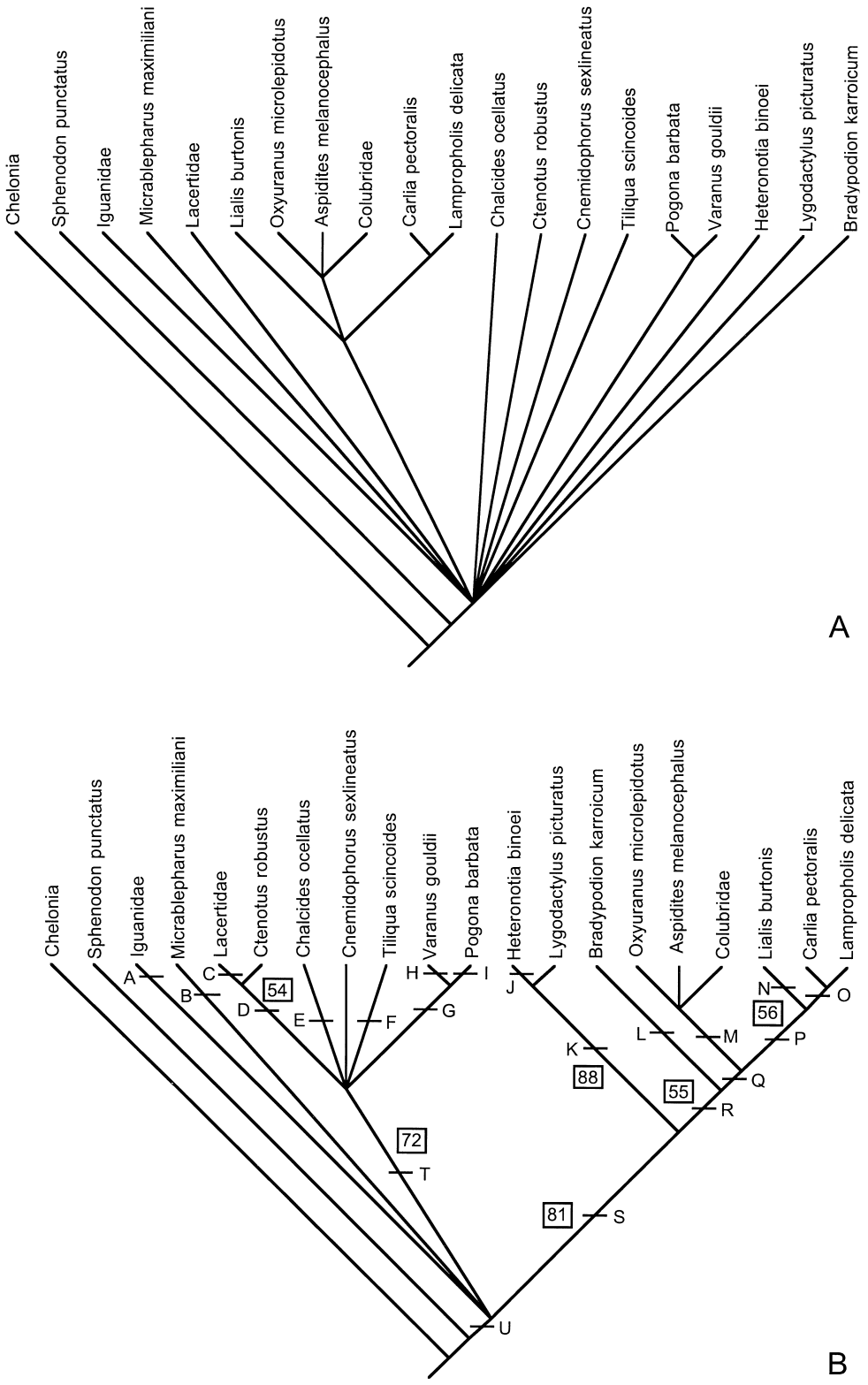

Fig. 4.—**A,** Strict consensus tree for 8733 equally parsimonious trees, derived from spermatozoa ultrastructure data listed in Tables 1 and 2.—**B,** 50% majority-rule consensus tree for the same 8733 trees. Numbers indicate the percentage of occurrence of clades among the equally parsimonious trees. Character-state changes in each labelled branch are listed in Table 3.

Table 3 Character-state changes in the 50% majority-rule tree depicted in Figure 4B. Reconstruction of character evolution according to ACCTRAN tracing. Unambiguous changes are underlined.

Node	Character	Change
A (Iguanidae)	8 (mitochondria shape)	1 → 2
B (*Micrablepharus maximiliani*)	5 (epinuclear lucent zone)	2 → 0
	7 (mitochondria in transverse section)	0 → 2
	8 (mitochondria shape)	1 → 4
C (Lacertidae)	9 (dense bodies)	1 → 5
	10 (dense bodies, if regular)	1 → 0
D	5 (epinuclear lucent zone)	2 → 1
E (*Chalcides ocellatus*)	10 (dense bodies, if regular)	1 → 3
F (*Tiliqua scincoides*)	5 (epinuclear lucent zone)	2 → 0
G	2	0 → 1
H (*Varanus gouldii*)	10 (dense bodies, if regular)	1 → 2
I (*Pogona barbata*)	7 (mitochondria in transverse section)	0 → 2
	8 (mitochondria shape)	1 → 3
J (*Heteronotia binoei*)	5 (epinuclear lucent zone)	2 → 0
K (Gekkonidae)	2 (perforatorial base plate)	0 → 2
	9 (dense bodies)	2 → 4
L (*Bradypodium karroicum*)	1 (acrosome in transverse section)	0 → 1
M (Serpentes)	5 (epinuclear lucent zone)	2 → 1
	6 (midpiece)	1 → 2
N (*Lialis burtonis*)	12 (nuclear shoulders)	0 → 2
O (*Eugongylus* species-group of	9 (dense bodies)	3 → 2
Scincidae)	15 (fibers 3 and 8)	0 → 1
	16 (multilaminar membranes)	1 → 0
P	2 (perforatorial base plate)	0 → 1
	3 (perforatorial tip)	0 → 1
	12 (nuclear shoulders)	1 → 0
	13 (nuclear shape)	0 → 1
Q	7 (mitochondria in transverse section)	0 → 1
	9 (dense bodies)	2 → 3
	16 (multilaminar membranes)	0 → 1
R	8 (mitochondria shape)	1 → 2
S	6 (midpiece)	0 → 1
	9 (dense bodies)	1 → 2
	10 (dense bodies, if regular)	1 → 0
T	1 (acrosome in transverse section)	0 → 1
U (Squamata)	4 (perforatoria number)	0 → 1
	5 (epinuclear lucent zone)	0 → 2
	8 (mitochondria shape)	0 → 1
	9 (dense bodies	0 → 1
	10 (dense bodies, if regular)	0 → 1
	11 (mitochondrial cristae)	0 → 1
	12 (nuclear shoulders)	0 → 1
	14 (endonuclear canal)	0 → 1
	17 (fibrous sheath)	0 → 1

Discussion

Ultrastructure of spermatozoa

The acrosome of *Micrablepharus maximiliani* exhibits the acrosome vesicle, the subacrosomal cone and the constricted nuclear tip, forming a tripartite pattern which is presumably plesiomorphic for amniotes and lissamphibians (Jamieson 1995a). The single perforatorium and the paracrystalline substructure of the subacrosomal cone of *M. maximiliani* are presumably synapomorphies of the Squamata (Jamieson 1995b). The acrosome is circular in transverse section throughout its length, as in the *Eugongylus* species-group (*Carlia* and *Lampropholis*) of the Scincidae (Jamieson and Scheltinga 1994; Jamieson *et al.* 1996), Gekkonidae (Furieri 1970; Jamieson *et al.* 1996), Pygopodidae (Jamieson *et al.* 1996), Iguanidae (Saita *et al.* 1988) and Serpentes (Oliver *et al.* 1996). The perforatorium of *M. maximiliani* is pointed at its anterior end and no basal plate was observed at its posterior end. In contrast, skinks of the *Eugongylus* species-group and the Pygopodidae display a square-ended perforatorial tip (Jamieson *et al.* 1996). As with *Micrablepharus*, the *Sphenomorphus* and *Egernia* species-groups of Scincidae (Furieri 1970; Jamieson *et al.* 1996), Lacertidae (Furieri 1970; Butler and Gabri 1984; Courtens and Depeiges, 1985),

Chamaeleonidae (Jamieson 1995b), Iguanidae (Saita *et al.* 1988) and Serpentes (Oliver *et al.* 1996) also lack the perforatorial basal plate.

Two nuclear traits are regarded as synapomorphic for the Squamata: the loss of the endonuclear canal and the presence of an epinuclear electron-lucent region (Jamieson 1995b). The spermatozoa of *Micrablepharus maximiliani* also lacks the endonuclear canal, but has no epinuclear electron-lucent space, like the skink *Tiliqua scincoides* (Jamieson and Scheltinga 1994) and the gecko *Heteronotia binoei* (Jamieson *et al.* 1996), what presumably is a reversal to the ancestral condition exhibited by *Sphenodon* and the Chelonia (Jamieson 1995b). The gently rounded nuclear shoulders, at the base of the tapered nuclear tip, in *M. maximiliani* sperm resembles the condition exhibited by most squamates (Jamieson 1995b). The basal nuclear fossa of *M. maximiliani* is dome-shaped, but it is not so well developed as in the sperm of the *Sphenomorphus* and *Egernia* species-group of skinks (Jamieson and Scheltinga 1993; Jamieson *et al.* 1996).

In the anterior portion of the midpiece, the proximal and distal centrioles are clearly observed in *Micrablepharus maximiliani*, a plesiomorphic condition in all tetrapods (Jamieson 1995a). As in other squamates, the sperm of *M. maximiliani* presents a short distal centriole, which forms the basal body of the axoneme and is penetrated by two central singlets from the axoneme (Jamieson 1995b; Jamieson *et al.* 1996; Oliver *et al.* 1996). *Micrablepharus maximiliani* presents dense material surrounding its distal centriole, a feature that has been reported in all amniotes (Jamieson *et al.* 1997). An electron-dense laminar structure was observed in *M. maximiliani*, extending from the pericentriolar apparatus, above the proximal centriole. Its presence has been clearly described in the *Sphenomorphus* species-group of skinks (Jamieson and Scheltinga 1993, 1994).

The short midpiece of *Micrablepharus maximiliani* sperm has been reported for the *Sphenomorphus* and *Egernia* species-group of Scincidae (Jamieson and Scheltinga 1993, 1994; Jamieson *et al.* 1996), Lacertidae (Furieri 1970; Butler and Gabri 1984; Courtens and Depeiges 1985), Teiidae (Newton and Trauth 1992), Agamidae (Oliver *et al.* 1996), Varanidae (Oliver *et al.* 1996) and Iguanidae (Saita *et al.* 1988). The mitochondria and dense bodies of *M. maximiliani* differ in shape and organization from those of other squamates studied to date. The mitochondria are trapezoid in longitudinal section, apparently arranged in spiral fashion around the fibrous sheath. Dense bodies lie in depressions of the mitochondrial cover, being in most sections separated from the fibrous sheath by mitochondria, and form regular rings that are not continuous in transverse sections. The arrangement of dense bodies in *M. maximiliani* most closely resembles that of *Pogona barbata*, where the ring structures are not continuous in transverse sections (Oliver *et al.* 1996).

The fibrous sheath in *Micrablepharus maximiliani* extends well into the midpiece, a synapomorphy of the Squamata (Jamieson 1995b). Nine peripheral dense fibers are associated with the nine doublets of the axoneme, and the peripheral fibers adjacent to doublets 3 and 8 are enlarged and detached from their respective doublets. These features are typical of all reptiles studied to date (Jamieson *et al,* 1997). Dense material is associated with one of the central microtubules of the distal centriole in *M. maximiliani*. This was also observed in snakes (Jamieson and Koehler 1994; Oliver *et al.* 1996), skinks (Jamieson and Scheltinga 1993, 1994), and geckos (Jamieson *et al.* 1996), and may be more widespread in squamates, depending upon appropriate sections of the distal centriole (Jamieson and Koehler 1994).

In *Micrablepharus maximiliani* the principal piece consists of the axoneme wrapped by the fibrous sheath, as in other amniotes (Jamieson 1995a), and the nine peripheral fibers are absent from the principal piece, as in other squamates (Jamieson 1995b).

Phylogeny of the Squamata

The addition of *Micrablepharus maximiliani* to the data set of Jamieson (1995b) basically produced two major effects: it significantly raised the number of optimal trees and lowered the resolution of both the strict and the 50% majority-rule consensus trees. Four groups, however, remained unaltered in the strict consensus tree after the addition of *M. maximiliani*: (1) *Pogona barbata* and *Varanus gouldii*; (2) Serpentes; (3) *Carlia pectoralis* and *Lampropholis delicata*; and (4) *Lialis burtonis*, Serpentes, and *C. pectoralis* and *L. delicata*.

Most-parsimonious trees depicting phylogenetic relationships among the Squamata, derived from spermatozoa ultrastructural characters, contain major areas of disagreement relative to trees produced from gross morphological characters (Estes *et al.* 1988), tongue morphology (Schwenk 1988), and limb musculature (Russel 1988). Major groups, such as the Iguania, Gekkota, Scincomorpha, and Anguimorpha, and families such as the Chamaeleonidae (*sensu* Frost and Etheridge 1989) and Scincidae, whose monophyly is supported by the three latter data sets, are not monophyletic in trees derived from the sperm ultrastructure data set.

Given the conflict between the trees supported by the sperm ultrastructure and the gross morphology data sets, it is reasonable to assume that at least one of the data sets is misleading, since there is just one tree of life. One could then conceive that, because the number of charaters and degree of support for the tree(s) derived from the morphology data sets surpass to a large extent those derived from the sperm ultrastructure data set, this latter data set is probably too noisy and contains little phylogenetic signal. Even though Jamieson (1995b) stated that the utility of spermatozoal ultrastructure as a source of characters for phylogenetic

analysis is well established', no one has explicitly tested his assertion.

A useful criterion for evaluating the phylogenetic content of characters is the analysis of tree-length skewness, as tree-length distributions with significant left skewness contain more phylogenetic signal than more symmetrical or right-skewed distributions (Hillis 1991; Huelsenbeck, 1991). The g_1 statistic is used to test for the skewness of frequency distributions: for a symmetrical distribution $g_1 = 0$, whereas a right-skewed distribution has a $g_1 > 0$ and a left-skewed distribution has a $g_1 < 0$ (Zar, 1984). Hillis (1991) pointed out that when testing for the skewness of tree-length distributions it is not appropriate to use the normal distribution as a null model, because the degree of expected departures from symmetry for a normal distribution decreases with increasing sample size, and sample size increases very rapidly with an increase in the number of taxa. Thus, he suggested that an empirically generated distribution of g_1 statistics provides a better means of testing for significant skewness, because no a priori assumptions about the shape of the distribution are made (Hillis, 1991). The skewness test has been severely criticized by Källersjö *et al.* (1992), who showed that under a particular set of circumstances (two hypothetical data sets) the skewness test can be misleading and that it can be more affected by the frequencies of states within characters than by congruence among characters. Further, they showed that the skewness test is insensitive to the number of characters. However, Källersjö *et al.* (1992) did not explore the issue of how likely the character-state distributions they presented can be observed in nature. This is still a largely unexplored issue but, apparently, the two hypothetical data sets presented by Källersjö *et al.* (1992) are so improbable that they will never be observed empirically under any tree model or under any model of character evolution and character sampling in which stochastic processes play a part (J. Lyons-Weiler, pers. comm.). The fact that one can, by intelligent design, create a set of conditions under which a given measure will fail, sheds little light on the general performance of that measure. For instance, Felsenstein (1978) has shown that under certain circumstances parsimony methods can be positively misleading. However, parsimony is still a dominant method in phylogenetic reconstruction. Every single method will have its assumptions violated at least occasionally or will perform poorly under some set of circumstances, but until it can be demonstrated how often this occurs, no arguments for or against it can be regarded as overly compelling (Maddison and Maddison 1992).

To test the null hypothesis that the squamate spermatozoa ultrastructure data set contains no phylogenetic signal, we constructed 100 data sets, each with 20 taxa and 17 characters (the same dimensions as the real data set), using the random data generator of MacClade v.3.06 (Maddison and Maddison 1992). Two states were allowed for each character, 0 and 1, each with a 0.5 probability of occurrence. Given the large number of possible unrooted, labelled trees for 20 taxa ($\approx 2.22 \times 10^{20}$), we generated 10 000 random trees from each of the 100 random data sets and calculated the g_1 value of each tree-length distribution using Paup vs. 3.0 s (Swofford 1991a) in order to produce an empirical distribution of g_1 statistics. We also generated a g_1 statistic from the squamate spermatozoa ultrastructure data, based on a random sample of 10 000 trees. The lower 5% and 1% of the empirical g_1 distribution were, respectively, –0.19 and –0.21 (Fig. 5A). This indicates that the g_1 statistic produced from the real data (–0.80) is highly significant and therefore sperm ultrastructure data does indeed contain significant phylogenetic signal (Fig. 5B).

Another possibility is that characters in each data set are affected by distinct stochastic processes, which lead to different rates of evolutionary change (de Queiroz *et al.* 1995). For instance, even though some ultrastructural characters seem rather conservative in terms of change, as the possession of a single perforatorium, linear mitochondrial cristae, absence of endonuclear canal, and a fibrous sheath that extends into the midpiece, members of the family with the highest number of species in the study matrix (Scincidae) are highly scattered in each of the best phylogenetic reconstructions, forming para-or polyphyletic groups (Fig. 4B). Among the two other families with more than one species in the study matrix, the chamaeleonids *Pogona barbata* and *Bradypodion karroicum* are also placed at very distant portions of the best trees (Fig. 4B). It is possible, as suggested by Jamieson (1995b), that some of these groups are not monophyletic, but we advance that the intrafamilial variability may be higher than currently thought. Therefore, spermatozoa ultrastructure characters might be more useful, as a source of phylogenetic information, at the generic or familial level and tree topology estimates derived from them might be rather incongruent with those derived from putatively more conservative morphological characters, because of heterogeneous rates of evolution. Additional studies are necessary to further our understanding on the levels of variability in spermatozoa ultrastructure characters across taxonomic categories.

Finally, we should also entertain the possibility that the heterogeneity between the spermatozoa ultrastructure and the morphological data sets is only apparent. Swofford (1991b) argued that the selection of trees for comparison is a critical issue in the evaluation of congruence. Selecting only the optimal trees for each data set results in the loss of all the uncertainty associated with the estimate of the tree. Hence, near-optimal trees should also be considered in the analysis of congruence. If the incongruence between the data sets is greater than that expected by chance, i.e. if the data sets can be regarded as independent, then individual data sets that are incompatible with others can be targeted for future studies concerning the sources of their significant heterogeneity (Miyamoto and Fitch 1995).

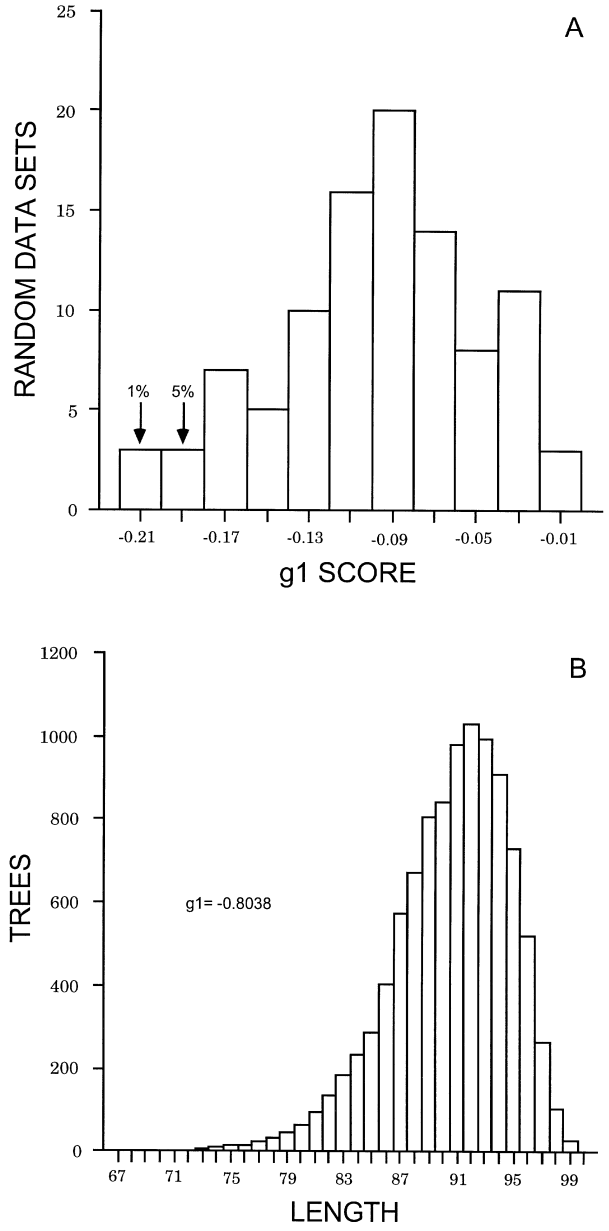

Fig. 5.—**A,** Distribution of skewness statistics (g_1) for tree-length distributions produced from 100 random data matrices. Arrows indicate the lower 1% and 5% critical values of the distribution. —**B,** Tree-length distribution of 10 000 random trees obtained from the spermatozoal ultrastructure data set of the Squamata.

Acknowledgements

We thank Ayrton K. Péres Jr. for assistance during field work and Gustavo H. C. Vieira for excellent technical assistance with laboratory work. We also thank Danny Eibye-Jacobsen and an anonymous reviewer for their insightful suggestions on an earlier version of the manuscript. The study was supported by CAPES, CNPq and FAPDF.

References

Barret, M., Donoghue, M. J. and Sober, E. 1991. Against consensus. – *Systematic Zoology* **40:** 486–493.

Butler, R. D. and Gabri, M. S. 1984. Structure and development of the sperm head in the lizard *Podarcis* (= *Lacerta*) *taurica*. – *Journal of Ultrastructure Research* **88:** 261–274.

Courtens, J. L. and Depeiges, A. 1985. Spermiogenesis of *Lacerta vivipara*. – *Journal of Ultrastructure Research* **90:** 203–220.

Estes, R., de Queiroz, K. and Gauthier, J. 1988. Phylogenetic relationships within Squamata. In Estes R. and Pregill G. (Eds): *Phylogenetic Relationships of the Lizard Families. Essays Commemorating Charles L. Camp*, pp. 119–281, Stanford University Press, Stanford, California.

Felsenstein, J. 1978. Cases in which parsimony or compatibility methods will be positively misleading. – *Systematic Zoology* **27:** 401–410.

Frost, D. R. and Etheridge, R. 1989. A phylogenetic analysis and taxonomy of iguanian lizards (Reptilia: Squamata). – *Miscellaneous Publications of the Museum of Natural History, University of Kansas* **81:** 1–65.

Furieri, P. 1970. Sperm morphology of some reptiles: Squamata and Chelonia. In Baccetti B. (Ed): *Comparative Spermatology*, pp. 115–131. Accademia Nazionale dei Lincei, Rome, Italy.

Hillis, D. M. 1991. Discriminating between phylogenetic signal and random noise in DNA sequences. In Miyamoto M. M. and Cracraft J. (Eds): *Phylogenetic Analysis of DNA Sequences*, pp. 278–294. Oxford University Press, New York, New York.

Huelsenbeck, J. P. 1991. Tree-length distribution skewness: an indicator of phylogenetic information. – *Systematic Zoology* **40:** 257–270.

Jamieson, B. G. M. 1987. *The Ultrastructure and Phylogeny of Insect Spermatozoa*. Cambridge University Press, Cambridge, UK.

Jamieson, B. G. M. 1991. *Fish Evolution and Systematics: Evidence from Spermatozoa*. Cambridge University Press, Cambridge, UK.

Jamieson, B. G. M. 1995a. Evolution of tetrapod spermatozoa with particular reference to amniotes. In Jamieson B. G. M., Ausio J. and Justine J. (Eds): *Advances in Spermatozoal Phylogeny and Taxonomy*, pp. 343–358. Muséum National d'Histoire Naturelle, Paris, France.

Jamieson, B. G. M. 1995b. The ultrastructure of spermatozoa of the Squamata (Reptilia) with phylogenetic considerations. In Jamieson B. G. M., Ausio J. and Justine J. (Eds): *Advances in Spermatozoal Phylogeny and Taxonomy*, pp. 359–383. Muséum National d'Histoire Naturelle, Paris, France.

Jamieson, B. G. M. and Koehler, L. 1994. The ultrastructure of the spermatozoon of the northern water snake, *Nerodia sipedon* (Colubridae, Serpentes), with phylogenetic considerations. – *Canadian Journal of Zoology* **72:** 1648–1652.

Jamieson, B. G. M., Oliver, S. C. and Scheltinga, D. M. 1996. The ultrastructure of spermatozoa of Squamata. I. Scincidae, Gekkonidae and Pygopodidae (Reptilia). – *Acta Zoologica (Stockholm)* **77:** 85–100.

Jamieson, B. G. M. and Scheltinga, D. M. 1993. The ultrastructure of spermatozoa of *Nangura spinosa* (Scincidae, Reptilia). – *Memoirs of the Queensland Museum* **34:** 169–179.

Jamieson, B. G. M. and Scheltinga, D. M. 1994. The ultrastructure of spermatozoa of the Australian skinks, *Ctenotus taeniolatus*, *Carlia pectoralis* and *Tiliqua scincoides scincoides* (Scincidae, Reptilia). – *Memoirs of the Queensland Museum* **37:** 181–193.

Jamieson, B. G. M., Scheltinga, D. M. and Tucker, A. D. 1997. The ultrastructure of spermatozoa of the Australian freshwater crocodile, *Crocodylus johnstoni* Krefft, 1873 (Crocodylidae, Reptilia). – *Journal of Submicroscopic Cytology and Pathology* **29:** 265–274.

Källersjo, M., Farris, J. S., Kluge, A. G. and Bult, C. 1992. Skewness and permutation. – *Cladistics* **8:** 275–287.

Maddison, W. P. and Maddison, D. R. 1992. *MacClade: Analysis of Phylogeny and Character Evolution, Version 3.04*. Sinauer Associates, Inc., Sunderland, Massachusetts.

Maddison, D. R., Maddison, W. P. 1996. The Tree of Life: A distributed Internet project containing information about phylogeny and biodiversity. Internet address: http: // phylogeny.arizona.edu/tree/phylogeny.html.

Miyamoto, M. M. 1985. Consensus cladograms and general classifications. – *Cladistics* **1:** 186–189.

Miyamoto, M. M. and Fitch, W. M. 1995. Testing species phylogenies and phylogenetic methods with congruence. – *Systematic Biology* **44:** 64–76.

Newton, D. W. and Trauth, S. E. 1992. Ultrastructure of the spermatozoon of the lizard *Cnemidophorus sexlineatus* (Sauria: Teiidae). – *Herpetologica* **48:** 330–343.

Oliver, S. C., Jamieson, B. G. M. and Scheltinga, D. M. 1996. The ultrastructure of spermatozoa of Squamata. II. Agamidae, Varanidae, Colubridae, Elapidae, and Boidae (Reptilia). – *Herpetologica* **52:** 216–241.

Presch, W. 1980. Evolutionary history of the South American microteiid lizards (Teiidae: Gymnophthalminae). – *Copeia* **1980:** 35–56.

Presch, W. 1983. The lizard family Teiidae: is it a monophyletic group? – *Zoological Journal of the Linnean Society* **77:** 189–197.

de Queiroz, A., Donoghue, M. J. and Kim, J. 1995. Separate versus combined analysis of phylogenetic evidence. – *Annual Review of Ecology and Systematics* **26:** 657–681.

Russel, A. P. 1988. Limb muscles in relation to lizard systematics: a reappraisal. In Estes R. and Pregill G. (Eds): *Phylogenetic Relationships of the Lizard Families. Essays Commemorating Charles L. Camp*, pp. 493–568. Stanford University Press, Stanford, California.

Saita, A., Comazzi, M. and Perrotta, E. 1988. New data at the E. M. on the spermiogenesis of *Iguana delicatissima* Laurent involving comparative significance. – *Acta Embriologiae et Morphologiae Experimentalis (New Series)* **9:** 105–114.

Schwenk, K. 1988. Comparative morphology of the lepidosaur tongue and its relevance to squamate phylogeny. In Estes R. and Pregill G. (Eds): *Phylogenetic Relationships of the Lizard Families. Essays Commemorating Charles L. Camp*, pp. 569–598. Stanford University Press, Stanford, California.

Swofford, D. L. 1991a. *Paup: Phylogenetic Analysis Using Parsimony*, Version 3.*0s*. Illinois Natural History Survey, Champaign, Illinois.

Swofford, D. L. 1991b. When are phylogeny estimates from molecular and morphological data sets incongruent? In Miyamoto M. M. and Cracraft J. (Eds): *Phylogenetic Analysis of DNA Sequences*, pp. 295–333. Oxford University Press, Oxford.

Zar, J. H. 1984. *Biostatistical Analysis*, 2nd edn. Prentice Hall, Inc., Englewood Cliffs, New Jersey.

